NUMERICAL SIMULATION OF 3D QUASI-HYDROSTATIC, FREE-SURFACE FLOWS

By Vincenzo Casulli[1] and Guus S. Stelling[2]

ABSTRACT: Numerical models that assume hydrostatic pressure are usually sufficiently accurate for applications in civil engineering where the vertical component of the velocity is relatively small. Nevertheless, the vertical momentum, and, hence, the nonhydrostatic pressure component, cannot be neglected when the bottom topography of the domain changes abruptly, as in cases of short waves, or when the flow is determined by strong density gradients. In this paper a numerical method for the three-dimensional (3D) quasi-hydrostatic, free-surface flows is outlined. The governing equations are the Reynolds-averaged Navier-Stokes equations with the pressure decomposed into the sum of a hydrostatic component and a hydrodynamic component. The momentum equations, the incompressibility condition, and the equation for the free surface are integrated by a time-splitting method in such a fashion that the resulting numerical solution is mass conservative and stable at a minimal computational cost. Several applications serve to illustrate the effect of the deviation from the hydrostatic pressure.

INTRODUCTION

Problems where the hydrostatic approximation is no longer valid include flows over rapidly varying slopes (such as near continental shelf edges) and short waves where the ratio of the vertical-to-horizontal scales of motion is not very small. One of the most popular numerical methods that successfully simulates free-surface flows for the Navier-Stokes equations is the marker-and-cell method developed by Harlow and Welch (1965). The marker-and-cell method has been improved in several ways (Bulgarelli et al. 1984; Tome and McKee 1994), but a severe stability restriction, relating the time step to the spatial discretization and to the free-surface wave speed, inhibits this method from being applied to three-dimensional (3D) geophysical flows with a sufficiently fine grid to resolve the small-scale nonhydrostatic component of the flow. The stability condition on the surface wave speed can be removed by making the rigid lid approximation (Cox 1984). The rigid lid approximation, however, does not allow for realistic propagation of surface waves, and thus, tidal flows cannot be simulated.

Explicit integration of the shallow-water equations is known to allow for a time step limited by the Courant condition based on fast gravity waves (Stelling 1983; Blumberg and Mellor 1987). To circumvent this condition implicit methods were initially derived based upon an ADI type of factorization for the barotropic pressure mode and the continuity equation (Leendertse 1967; Stelling 1983), and were later based upon fully implicit integration of these modes (Benqué et al. 1982; Wilders et al. 1988; Casulli 1990). These methods can be extended to 3D models, based upon the hydrostatic pressure assumption (Madala and Piacsek 1977; Leendertse 1989; de Goede 1991; Casulli and Cheng 1992; Stelling and Leendertse 1992; Casulli and Cattani 1994).

This paper describes how an extension can be constructed within the aforementioned computational framework that allows numerical integration of the full Reynolds-averaged Navier-Stokes equations for simulating large-scale nonhydrostatic flows (Casulli 1995; Casulli and Stelling 1996; Mahadevan et al. 1996a,b). This is achieved by a fractional step method where the hydrostatic and the hydrodynamic component of the pressure are considered separately. The resulting algorithm is relatively simple, numerically stable even at large Courant numbers, and suitable for simulations of complex 3D flows using fine spatial resolution and relatively large time steps. Moreover, when the vertical momentum is neglected, the hydrostatic solution is produced as a particular case.

GOVERNING EQUATIONS

The governing 3D, primitive variable equations describing the free-surface flows can be derived from the Navier-Stokes equations after Reynolds averaging. Such equations express the physical principle of conservation of mass and momentum. The momentum equations for an incompressible fluid have the following form (Pedlosky 1979):

$$\rho\left(\frac{\partial u}{\partial t}+u\frac{\partial u}{\partial x}+v\frac{\partial u}{\partial y}+w\frac{\partial u}{\partial z}\right)=-\frac{\partial p}{\partial x}+\mu^h\left(\frac{\partial^2 u}{\partial x^2}+\frac{\partial^2 u}{\partial y^2}\right)+\frac{\partial}{\partial z}\left(\mu^v\frac{\partial u}{\partial z}\right)+\rho f v \tag{1}$$

$$\rho\left(\frac{\partial v}{\partial t}+u\frac{\partial v}{\partial x}+v\frac{\partial v}{\partial y}+w\frac{\partial v}{\partial z}\right)=-\frac{\partial p}{\partial y}+\mu^h\left(\frac{\partial^2 v}{\partial x^2}+\frac{\partial^2 v}{\partial y^2}\right)+\frac{\partial}{\partial z}\left(\mu^v\frac{\partial v}{\partial z}\right)-\rho f u \tag{2}$$

$$\rho\left(\frac{\partial w}{\partial t}+u\frac{\partial w}{\partial x}+v\frac{\partial w}{\partial y}+w\frac{\partial w}{\partial z}\right)=-\frac{\partial p}{\partial z}+\mu^h\left(\frac{\partial^2 w}{\partial x^2}+\frac{\partial^2 w}{\partial y^2}\right)+\frac{\partial}{\partial z}\left(\mu^v\frac{\partial w}{\partial z}\right)-\rho g \tag{3}$$

where $u(x, y, z, t)$, $v(x, y, z, t)$, and $w(x, y, z, t)$ = velocity components in the horizontal x, y and vertical z-direction; t = time; $p(x, y, z, t)$ = pressure; g = gravitational acceleration; ρ = fluid density; and μ^h and μ^v = coefficients of horizontal and vertical eddy viscosity, respectively. For applications to mesoscale oceanic flows the vertical component of the Coriolis acceleration should also be incorporated in (1)–(3) (Mahadevan et al. 1996a).

The fluid density ρ is specified by an equation of state $\rho = \rho(T, S)$, where T and S denote the temperature and the salinity, respectively. If either the temperature or the salinity concentration cannot be assumed constant, a transport equation for T or S must also be given as follows:

[1]Prof., Dept. of Civ. and Envir. Engrg., Univ. of Trento, 38050 Mesiano di Povo (Trento), Italy, and Consultant, Centro Internazionale per la Ricerca Matematica—Istituto Trentino di Cultura, 38050 Povo (Trento), Italy.

[2]Sr. Sci., Delft Hydraulics, P.O. Box 177, 2600 MH Delft, The Netherlands and Prof., Delft Univ. of Technol., Facu. of Civ. Engrg., P.O. Box 5046, 2600 GA Delft, The Netherlands.

Note. Discussion open until December 1, 1998. To extend the closing date one month, a written request must be filed with the ASCE Manager of Journals. The manuscript for this paper was submitted for review and possible publication on December 3, 1996. This paper is part of the *Journal of Hydraulic Engineering*, Vol. 124, No. 7, July, 1998. ©ASCE, ISSN 0733-9429/98/0007-0678–0686/$8.00 + $.50 per page. Paper No. 14720.

$$\frac{\partial c}{\partial t} + u\frac{\partial c}{\partial x} + v\frac{\partial c}{\partial y} + w\frac{\partial c}{\partial z} = \nu_c^h\left(\frac{\partial^2 c}{\partial x^2} + \frac{\partial^2 c}{\partial y^2}\right) + \frac{\partial}{\partial z}\left(\nu_c^v\frac{\partial c}{\partial z}\right) \quad (4)$$

where $c = T, S$; and ν_c^h and ν_c^v = coefficients of horizontal and vertical eddy diffusivity, respectively. Here, for simplicity only, the horizontal eddy diffusivity coefficient is assumed to be constant.

By denoting with $\eta(x, y, t)$ the free surface measured from the undisturbed water surface, the pressure $p(x, y, z, t)$ in (1)–(3) can be decomposed into the sum of a hydrostatic component and a hydrodynamic component. The hydrostatic pressure component is determined from the vertical momentum equation (3) by neglecting the convective and the viscous acceleration terms. Additionally, by using the Leibnitz integration rule, the hydrostatic pressure gradient can be split into the barotropic and the baroclinic components as follows:

$$\nabla p_h(x, y, z, t) = g\rho(x, y, \eta, t)\nabla\eta(x, y, t) + g\int_z^\eta \nabla\rho(x, y, \xi, t)\, d\xi \quad (5)$$

The atmospheric pressure term is usually prescribed and, for simplicity only, is assumed to be constant. Thus, the momentum equations (1)–(3), after the Boussinesq approximation, can also be written as

$$\frac{\partial u}{\partial t} + u\frac{\partial u}{\partial x} + v\frac{\partial u}{\partial y} + w\frac{\partial u}{\partial z} = -g\frac{\partial\eta}{\partial x} - \frac{g}{\rho_0}\int_z^\eta \frac{\partial\rho}{\partial x}\, d\xi - \frac{\partial q}{\partial x} + \nu^h\left(\frac{\partial^2 u}{\partial x^2} + \frac{\partial^2 u}{\partial y^2}\right) + \frac{\partial}{\partial z}\left(\nu^v\frac{\partial u}{\partial z}\right) + fv \quad (6)$$

$$\frac{\partial v}{\partial t} + u\frac{\partial v}{\partial x} + v\frac{\partial v}{\partial y} + w\frac{\partial v}{\partial z} = -g\frac{\partial\eta}{\partial y} - \frac{g}{\rho_0}\int_z^\eta \frac{\partial\rho}{\partial y}\, d\xi - \frac{\partial q}{\partial y} + \nu^h\left(\frac{\partial^2 v}{\partial x^2} + \frac{\partial^2 v}{\partial y^2}\right) + \frac{\partial}{\partial z}\left(\nu^v\frac{\partial v}{\partial z}\right) - fu \quad (7)$$

$$\frac{\partial w}{\partial t} + u\frac{\partial w}{\partial x} + v\frac{\partial w}{\partial y} + w\frac{\partial w}{\partial z} = -\frac{\partial q}{\partial z} + \nu^h\left(\frac{\partial^2 w}{\partial x^2} + \frac{\partial^2 w}{\partial y^2}\right) + \frac{\partial}{\partial z}\left(\nu^v\frac{\partial w}{\partial z}\right) \quad (8)$$

where q = normalized hydrodynamic pressure that is the deviation from the hydrostatic pressure divided by the constant reference density ρ_0; and ν^h and ν^v = kinematic eddy viscosity coefficients.

The conservation of volume is expressed by the following incompressibility condition:

$$\frac{\partial u}{\partial x} + \frac{\partial v}{\partial y} + \frac{\partial w}{\partial z} = 0 \quad (9)$$

Integrating the continuity equation (9) over the depth and using a kinematic condition at the free surface leads to the following free-surface equation:

$$\frac{\partial\eta}{\partial t} + \frac{\partial}{\partial x}\left[\int_{-h}^\eta u\, dz\right] + \frac{\partial}{\partial y}\left[\int_{-h}^\eta v\, dz\right] = 0 \quad (10)$$

where $h(x, y)$ = water depth measured from the undisturbed water surface. When the rigid lid approximation is made, $\eta(x, y, t)$ is no longer a function of time and (10) is not needed. On the other hand, when the hydrostatic approximation is made, (8) is neglected and $q(x, y, z, t) = 0$ is assumed throughout. In this latter case the hydrodynamic component of the pressure is assumed not to have any affect on the resulting circulation.

The boundary conditions at the free surface are specified by prescribing the wind stresses as

$$\nu^v\frac{\partial u}{\partial z} = \gamma_T(u_a - u); \quad \nu^v\frac{\partial v}{\partial z} = \gamma_T(v_a - v) \quad (11a,b)$$

where γ_T = nonnegative wind stress coefficient; and u_a and v_a = prescribed wind velocity components in the x- and y-directions, respectively. At the bed, the bottom friction is specified by

$$\nu^v\frac{\partial u}{\partial z} = \gamma_B u; \quad \nu^v\frac{\partial v}{\partial z} = \gamma_B v \quad (12a,b)$$

where γ_B = nonnegative bottom friction coefficient. Typically, γ_B can be derived from any turbulent boundary-layer assumption. The vertical eddy viscosity coefficient ν^v can be determined from an appropriate turbulence closure model that is beyond the scope of the present investigation. Here, it will only be assumed that ν^v is nonnegative everywhere.

NUMERICAL APPROXIMATION

To obtain an efficient numerical method whose stability is independent of the free-surface wave speed, wind stress, bottom friction, and vertical eddy viscosity, a fractional step scheme is derived. In the first step the hydrodynamic pressure is neglected and the gradient of surface elevation in the horizontal momentum equations (6) and (7) and the velocity in the free-surface equation (10) are discretized by the θ-method (Casulli and Cattani 1994). Moreover, for stability, the vertical viscosity terms will be discretized implicitly. In the second step the intermediate velocity computed in the first step is corrected by adding the hydrodynamic pressure terms that are calculated in such a fashion that the resulting velocity field is divergence free throughout the computational domain.

The physical domain is subdivided into $N_x N_y N_z$ rectangular boxes of length Δx, width Δy, and height $\Delta z_k = z_{k+1/2} - z_{k-1/2}$, respectively, where $z_{k\pm1/2}$ are given level surfaces. Each box is numbered at its center with indices i, j, and k. The discrete u velocity is then defined at half integer i and integers j and k; v is defined at integers i, k and half integer j; w is defined at integers i, j and half integer k; q is defined at integers i, j, and k. Finally, η is defined at integer i, j. The water depth $h(x, y)$ is specified at the u and v horizontal grid points.

First Step: Hydrostatic Pressure

The first step of calculations is performed by neglecting the hydrodynamic pressure terms in the momentum equations (6)–(8). The resulting velocity field at the new time level is not yet final and will be denoted by $\tilde{u}$, $\tilde{v}$, and $\tilde{w}$. A semi-implicit discretization for the momentum equations (6)–(8) takes the following form:

$$\tilde{u}^{n+1}_{i+1/2,j,k} = Fu^n_{i+1/2,j,k} - g\frac{\Delta t}{\Delta x}[\theta(\eta^{n+1}_{i+1,j} - \eta^{n+1}_{i,j}) + (1-\theta)(\eta^n_{i+1,j} - \eta^n_{i,j})] - g\frac{\Delta t}{\rho_0\Delta x}\left[\sum_{m=k}^{N_z}\Delta z^n_{i+1/2,j,m}(\rho^n_{i+1,j,m} - \rho^n_{i,j,m}) - \Delta z^n_{i+1/2,j,k}\frac{\rho^n_{i+1,j,k} - \rho^n_{i,j,k}}{2}\right] + \Delta t\frac{\nu^v_{k+1/2}\dfrac{\tilde{u}^{n+1}_{i+1/2,j,k+1} - \tilde{u}^{n+1}_{i+1/2,j,k}}{\Delta z^n_{i+1/2,j,k+1/2}} - \nu^v_{k-1/2}\dfrac{\tilde{u}^{n+1}_{i+1/2,j,k} - \tilde{u}^{n+1}_{i+1/2,j,k-1}}{\Delta z^n_{i+1/2,j,k-1/2}}}{\Delta z^n_{i+1/2,j,k}} \quad (13)$$

$$\tilde{v}^{n+1}_{i,j+1/2,k} = Fv^n_{i,j+1/2,k} - g\frac{\Delta t}{\Delta y}[\theta(\eta^{n+1}_{i,j+1} - \eta^{n+1}_{i,j}) + (1-\theta)(\eta^n_{i,j+1} - \eta^n_{i,j})] - g\frac{\Delta t}{\rho_0\Delta y}\left[\sum_{m=k}^{N_z}\Delta z^n_{i,j+1/2,m}(\rho^n_{i,j+1,m} - \rho^n_{i,j,m})\right.$$

$$- \Delta z^n_{i,j+1/2,k} \frac{\rho^n_{i,j+1,k} - \rho^n_{i,j,k}}{2}\Bigg]$$

$$+ \Delta t \frac{\nu^v_{k+1/2} \dfrac{\tilde{v}^{n+1}_{i,j+1/2,k+1} - \tilde{v}^{n+1}_{i,j+1/2,k}}{\Delta z^n_{i,j+1/2,k+1/2}} - \nu^v_{k-1/2} \dfrac{\tilde{v}^{n+1}_{i,j+1/2,k} - \tilde{v}^{n+1}_{i,j+1/2,k-1}}{\Delta z^n_{i,j+1/2,k-1/2}}}{\Delta z^n_{i,j+1/2,k}} \tag{14}$$

$$\tilde{w}^{n+1}_{i,j,k+1/2} = F w^n_{i,j,k+1/2}$$

$$+ \Delta t \frac{\nu^v_{k+1} \dfrac{\tilde{w}^{n+1}_{i,j,k+3/2} - \tilde{w}^{n+1}_{i,j,k+1/2}}{\Delta z^n_{i,j,k+1}} - \nu^v_k \dfrac{\tilde{w}^{n+1}_{i,j,k+1/2} - \tilde{w}^{n+1}_{i,j,k-1/2}}{\Delta z^n_{i,j,k}}}{\Delta z^n_{i,j,k+1/2}} \tag{15}$$

where Δz is usually defined as the distance between two consecutive level surfaces except near the bottom and near the free surface where Δz is the distance between a level surface and bottom or free surface, respectively. In general, Δz depends on the spatial location and, near the free surface, also depends on the time step. The vertical space increment Δz is also allowed to vanish to account for variable geometries and for the wetting and drying of tidal flats. Of course, the corresponding momentum equations (13), (14), or (15) are not defined at a grid point characterized by $\Delta z = 0$. In (13)–(15), F is a finite difference operator that includes the explicit discretization of the convective terms, the horizontal viscosity terms, and the Coriolis acceleration. Eqs. (13)–(15) also include appropriate discretizations of the boundary conditions (11) and (12) at the free surface and at the bottom (Casulli and Cheng 1992).

For each i, j, the set of (15) form a linear, tridiagonal system of $N_z - 1$ equations with unknowns $\tilde{w}^{n+1}_{i,j,k+1/2}$, $k = 1, 2, \ldots, N_z - 1$. The coefficient matrix of these systems is symmetric and positive definite. Thus, the intermediate vertical component of the velocity can be determined uniquely and efficiently by a direct method. Eqs. (13) and (14) also constitute a set of linear tridiagonal systems that are coupled to the unknown water surface elevation η^{n+1}. To determine $\eta^{n+1}_{i,j}$, and for numerical stability, the intermediate velocity field is required to satisfy, for each i, j, the discrete analog of the free-surface equation (10)

$$\eta^{n+1}_{i,j} = \eta^n_{i,j} - \theta \frac{\Delta t}{\Delta x}\left[\sum_{k=1}^{N_z} \Delta z^n_{i+1/2,j,k} \tilde{u}^{n+1}_{i+1/2,j,k} - \sum_{k=1}^{N_z} \Delta z^n_{i-1/2,j,k} \tilde{u}^{n+1}_{i-1/2,j,k}\right]$$

$$- \theta \frac{\Delta t}{\Delta y}\left[\sum_{k=1}^{N_z} \Delta z^n_{i,j+1/2,k} \tilde{v}^{n+1}_{i,j+1/2,k} - \sum_{k=1}^{N_z} \Delta z^n_{i,j-1/2,k} \tilde{v}^{n+1}_{i,j-1/2,k}\right]$$

$$- (1 - \theta) \frac{\Delta t}{\Delta x}\left[\sum_{k=1}^{N_z} \Delta z^n_{i+1/2,j,k} u^n_{i+1/2,j,k} - \sum_{k=1}^{N_z} \Delta z^n_{i-1/2,j,k} u^n_{i-1/2,j,k}\right]$$

$$- (1 - \theta) \frac{\Delta t}{\Delta y}\left[\sum_{k=1}^{N_z} \Delta z^n_{i,j+1/2,k} v^n_{i,j+1/2,k} - \sum_{k=1}^{N_z} \Delta z^n_{i,j-1/2,k} v^n_{i,j-1/2,k}\right] \tag{16}$$

Eqs. (13), (14), and (16) now constitute a large linear system of $N_x N_y (2N_z + 1)$ equations with unknowns $\tilde{u}^{n+1}_{i+1/2,j,k}$, $\tilde{v}^{n+1}_{i,j+1/2,k}$, and $\eta^{n+1}_{i,j}$. For computational convenience this system is first reduced to a smaller, five diagonal system of only $N_x N_y$ equations in which $\eta^{n+1}_{i,j}$ are the only unknowns. Specifically, upon multiplication by $\Delta z^n_{i+1/2,j,k}$ and $\Delta z^n_{i,j+1/2,k}$, (13), (14), and (16) are first written in matrix notation as

$$\mathbf{A}^n_{i+1/2,j} \tilde{\mathbf{U}}^{n+1}_{i+1/2,j} = \mathbf{G}^n_{i+1/2,j} - \theta g \frac{\Delta t}{\Delta x}(\eta^{n+1}_{i+1,j} - \eta^{n+1}_{i,j}) \Delta \mathbf{Z}^n_{i+1/2,j} \tag{17}$$

$$\mathbf{A}^n_{i,j+1/2} \tilde{\mathbf{V}}^{n+1}_{i,j+1/2} = \mathbf{G}^n_{i,j+1/2} - \theta g \frac{\Delta t}{\Delta y}(\eta^{n+1}_{i,j+1} - \eta^{n+1}_{i,j}) \Delta \mathbf{Z}^n_{i,j+1/2} \tag{18}$$

$$\eta^{n+1}_{i,j} = \delta^n_{i,j} - \theta \frac{\Delta t}{\Delta x}[(\Delta \mathbf{Z}^n_{i+1/2,j})^T \tilde{\mathbf{U}}^{n+1}_{i+1/2,j} - (\Delta \mathbf{Z}^n_{i-1/2,j})^T \tilde{\mathbf{U}}^{n+1}_{i-1/2,j}]$$

$$- \theta \frac{\Delta t}{\Delta y}[(\Delta \mathbf{Z}^n_{i,j+1/2})^T \tilde{\mathbf{V}}^{n+1}_{i,j+1/2} - (\Delta \mathbf{Z}^n_{i,j-1/2})^T \tilde{\mathbf{V}}^{n+1}_{i,j-1/2}] \tag{19}$$

where $\tilde{\mathbf{U}}^{n+1}_{i+1/2,j}$ and $\tilde{\mathbf{V}}^{n+1}_{i,j+1/2}$ = vectors of N_z components u and v at the specified horizontal location; $\mathbf{A}$ = symmetric, positive definite, tridiagonal matrix of order N_z; $\mathbf{G}^n_{i+1/2,j}$ and $\mathbf{G}^n_{i,j+1/2}$ = vectors containing all the explicit terms in (13) and (14), respectively; $\delta^n_{i,j}$ contains all the explicit terms in (16); and, finally, $\Delta \mathbf{Z}$ denotes a vector of N_z components $\Delta z^n_{i+1/2,j,k}$ and $\Delta z^n_{i,j+1/2,k}$. Then, formal substitution of the expressions for $\tilde{\mathbf{U}}^{n+1}_{i+1/2,j}$ and $\tilde{\mathbf{V}}^{n+1}_{i,j+1/2}$ from (17) and (18) into (19) yields

$$\eta^{n+1}_{i,j} - g\theta^2 \frac{\Delta t^2}{\Delta x^2}\{[(\Delta \mathbf{Z})^T \mathbf{A}^{-1} \Delta \mathbf{Z}]^n_{i+1/2,j}(\eta^{n+1}_{i+1,j} - \eta^{n+1}_{i,j})$$

$$- [(\Delta \mathbf{Z})^T \mathbf{A}^{-1} \Delta \mathbf{Z}]^n_{i-1/2,j}(\eta^{n+1}_{i,j} - \eta^{n+1}_{i-1,j})\}$$

$$- g\theta^2 \frac{\Delta t^2}{\Delta y^2}\{[(\Delta \mathbf{Z})^T \mathbf{A}^{-1} \Delta \mathbf{Z}]^n_{i,j+1/2}(\eta^{n+1}_{i,j+1} - \eta^{n+1}_{i,j})$$

$$- [(\Delta \mathbf{Z})^T \mathbf{A}^{-1} \Delta \mathbf{Z}]^n_{i,j-1/2}(\eta^{n+1}_{i,j} - \eta^{n+1}_{i,j-1})\}$$

$$= \delta^n_{i,j} - \frac{\Delta t}{\Delta x}\{[(\Delta \mathbf{Z})^T \mathbf{A}^{-1} \mathbf{G}]^n_{i+1/2,j} - [(\Delta \mathbf{Z})^T \mathbf{A}^{-1} \mathbf{G}]^n_{i-1/2,j}\}$$

$$- \frac{\Delta t}{\Delta y}\{[(\Delta \mathbf{Z})^T \mathbf{A}^{-1} \mathbf{G}]^n_{i,j+1/2} - [(\Delta \mathbf{Z})^T \mathbf{A}^{-1} \mathbf{G}]^n_{i,j-1/2}\} \tag{20}$$

Since the matrix $\mathbf{A}$ is an M-matrix, $\mathbf{A}^{-1}$ has nonnegative elements everywhere. Therefore the quantity $(\Delta \mathbf{Z})^T \mathbf{A}^{-1} \Delta \mathbf{Z}$ is nonnegative everywhere. Hence, (20) constitutes a five diagonal system of $N_x N_y$ equations for the unknowns $\eta^{n+1}_{i,j}$. This system is symmetric and positive definite; thus (20) has a unique solution that can be efficiently determined by a preconditioned conjugate gradient method. Once the new free-surface location has been determined, (17) and (18) constitute a set of $2N_x N_y$ tridiagonal systems that can be easily solved to determine $\tilde{u}^{n+1}_{i+1/2,j,k}$ and $\tilde{v}^{n+1}_{i,j+1/2,k}$ throughout the computational domain. Next, the new vertical increments Δz can be updated to account for the new free-surface location.

Second Step: Hydrodynamic Pressure

In the second step of calculations the new velocity field $u^{n+1}_{i+1/2,j,k}$, $v^{n+1}_{i,j+1/2,k}$, and $w^{n+1}_{i,j,k+1/2}$ is computed by correcting the intermediate velocity field with the gradient of the hydrodynamic pressure. The new hydrodynamic pressure is thus determined by requiring that the new velocity field is divergence free. Specifically, the discrete momentum equations are taken to be

$$u^{n+1}_{i+1/2,j,k} = \tilde{u}^{n+1}_{i+1/2,j,k} - \frac{\Delta t}{\Delta x}(q^{n+1}_{i+1,j,k} - q^{n+1}_{i,j,k}) \tag{21}$$

$$v^{n+1}_{i,j+1/2,k} = \tilde{v}^{n+1}_{i,j+1/2,k} - \frac{\Delta t}{\Delta y}(q^{n+1}_{i,j+1,k} - q^{n+1}_{i,j,k}) \tag{22}$$

$$w^{n+1}_{i,j,k+1/2} = \tilde{w}^{n+1}_{i,j,k+1/2} - \frac{\Delta t}{\Delta z^{n+1}_{i,j,k+1/2}}(q^{n+1}_{i,j,k+1} - q^{n+1}_{i,j,k}) \tag{23}$$

and, in each computational box laying below the free surface, the discretized incompressibility condition is taken to be

$$\frac{u^{n+1}_{i+1/2,j,k} \Delta z^{n+1}_{i+1/2,j,k} - u^{n+1}_{i-1/2,j,k} \Delta z^{n+1}_{i-1/2,j,k}}{\Delta x}$$

$$+ \frac{v^{n+1}_{i,j+1/2,k} \Delta z^{n+1}_{i,j+1/2,k} - v^{n+1}_{i,j-1/2,k} \Delta z^{n+1}_{i,j-1/2,k}}{\Delta y}$$

$$+ w^{n+1}_{i,j,k+1/2} - w^{n+1}_{i,j,k-1/2} = 0 \tag{24}$$

Eqs. (21)–(24) constitute a linear system with $2N_xN_y(2N_z - 1)$ equations and $2N_xN_y(2N_z - 1)$ unknowns $u^{n+1}_{i+1/2,j,k}$, $v^{n+1}_{i,j+1/2,k}$, $w^{n+1}_{i,j,k+1/2}$ and $q^{n+1}_{i,j,k}$ throughout the computational domain. This system can be reduced to a smaller one by substituting the expressions for the new velocities from (21)–(23) into the incompressibility equation (24). There results the following finite difference Poisson equation for the hydrodynamic pressure:

$$\Delta t\left[\frac{(q^{n+1}_{i+1,j,k}-q^{n+1}_{i,j,k})\Delta z^{n+1}_{i+1/2,j,k}-(q^{n+1}_{i,j,k}-q^{n+1}_{i-1,j,k})\Delta z^{n+1}_{i-1/2,j,k}}{\Delta x^2}\right.$$
$$+\frac{(q^{n+1}_{i,j+1,k}-q^{n+1}_{i,j,k})\Delta z^{n+1}_{i,j+1/2,k}-(q^{n+1}_{i,j,k}-q^{n+1}_{i,j-1,k})\Delta z^{n+1}_{i,j-1/2,k}}{\Delta y^2}$$
$$\left.+\frac{q^{n+1}_{i,j,k+1}-q^{n+1}_{i,j,k}}{\Delta z^{n+1}_{i,j,k+1/2}}-\frac{q^{n+1}_{i,j,k}-q^{n+1}_{i,j,k-1}}{\Delta z^{n+1}_{i,j,k-1/2}}\right]$$
$$=\frac{\tilde{u}^{n+1}_{i+1/2,j,k}\Delta z^{n+1}_{i+1/2,j,k}-\tilde{u}^{n+1}_{i-1/2,j,k}\Delta z^{n+1}_{i-1/2,j,k}}{\Delta x}$$
$$+\frac{\tilde{v}^{n+1}_{i,j+1/2,k}\Delta z^{n+1}_{i,j+1/2,k}-\tilde{v}^{n+1}_{i,j-1/2,k}\Delta z^{n+1}_{i,j-1/2,k}}{\Delta y}$$
$$+\tilde{w}^{n+1}_{i,j,k+1/2}-\tilde{w}^{n+1}_{i,j,k-1/2} \tag{25}$$

Eq. (25) forms a seven diagonal linear system of $N_xN_y(N_z - 1)$ equations and $N_xN_y(N_z - 1)$ unknowns $q^{n+1}_{i,j,k}$ that is symmetric and positive definite. Thus, (25) can be solved iteratively by the preconditioned conjugate gradient method. Once the hydrodynamic pressure is computed, the corresponding velocity field is readily determined from (21)–(23).

At the solid impenetrable boundaries, the condition of zero normal flow is imposed through (21)–(23), which translates to Neumann type of boundary conditions on (25). At the free surface, the Dirichlet type of boundary conditions on (25) are specified by setting the hydrodynamic pressure $q^{n+1}_{i,j,k}$ equal to zero. At the open boundaries either the normal velocity or the nonhydrostatic pressure should be specified. Accordingly, this translates into the Neumann or Dirichlet type of boundary condition for (25). Often, however, neither the normal velocity nor the pressure are available; in these cases the hydrostatic approximation ($q = 0$) can be assumed at the open boundaries.

In summary, the numerical solution of the free-surface Reynolds-averaged Navier-Stokes equations at each time step is obtained by solving a sequence of linear systems to obtain $\eta^{n+1}_{i,j}$, $\tilde{u}^{n+1}_{i+1/2,j,k}$, $\tilde{v}^{n+1}_{i,j+1/2,k}$, $\tilde{w}^{n+1}_{i,j,k+1/2}$, $q^{n+1}_{i,j,k}$, $u^{n+1}_{i+1/2,j,k}$, $v^{n+1}_{i,j+1/2,k}$, and $w^{n+1}_{i,j,k+1/2}$, respectively. The sequence of linear systems is as follows:

1. The five diagonal system of (20) is solved for $\eta^{n+1}_{i,j}$.
2. For each i, j, the tridiagonal systems of (13), (14), and (15) are solved for $\tilde{u}^{n+1}_{i+1/2,j,k}$, $\tilde{v}^{n+1}_{i,j+1/2,k}$, and $\tilde{w}^{n+1}_{i,j,k+1/2}$, respectively.
3. The hydrodynamic pressure $q^{n+1}_{i,j,k}$ is determined by solving the seven diagonal system of (25).
4. The final velocity field $u^{n+1}_{i+1/2,j,k}$, $v^{n+1}_{i,j+1/2,k}$, and $w^{n+1}_{i,j,k+1/2}$ is obtained explicitly from (21)–(23).

Each of the aforementioned systems is symmetric and positive definite; thus, the existence and uniqueness of the numerical solution is assured.

Finally, when the density cannot be assumed to be constant, the transport equation (4) must also be solved numerically by using a semi-implicit Eulerian-Lagrangian method or any conservative semi-implicit scheme.

PROPERTIES OF METHOD

In geophysical applications the flow domain is characterized by having a vertical scale much smaller than the horizontal scale; thus, the vertical increments Δz are much smaller than both Δx and Δy. In terms of the seven diagonal linear system (25) the preceding consideration implies a stronger tie among the vertical between the $q^{n+1}_{i,j,k}$ that results into a faster convergence of the iterative method. Moreover, in geophysical applications the hydrostatic pressure is usually a good approximation for the total pressure. This means that the hydrodynamic pressure is close to zero almost everywhere and the variations of the hydrodynamic pressure are some order of magnitude smaller than the variations of the hydrostatic pressure. For this reason, rather than using a more direct approach to compute for the total pressure out of a seven diagonal system, more efficiency is gained from computing a rapidly varying hydrostatic pressure from several iterations on a five diagonal system. Next, the slowly varying hydrodynamic pressure is obtained from a larger seven diagonal system, but in only a few iterations. Thus, although fully nonhydrostatic flows can be simulated by the present model, the model's applicability to flows where the hydrodynamic pressure represents a small perturbation is particularly effective. These flows are defined as quasi-hydrostatic flows.

As it may be noted, the free-surface is calculated before the correction for the hydrodynamic pressure. Thus, the model accuracy is limited by the fact that the hydrodynamic pressure is assumed to be small compared with the hydrostatic pressure.

If the discrete vertical momentum equation (15) is neglected, the resulting system admits an infinity of solutions. One of these solutions can be chosen in such a way that the intermediate velocity field is exactly discrete divergence free, that is, $\tilde{w}^{n+1}_{i,j,1/2} = 0$ and

$$\tilde{w}^{n+1}_{i,j,k+1/2}=\tilde{w}^{n+1}_{i,j,k-1/2}-\frac{\tilde{u}^{n+1}_{i+1/2,j,k}\Delta z^{n+1}_{i+1/2,j,k}-\tilde{u}^{n+1}_{i-1/2,j,k}\Delta z^{n+1}_{i-1/2,j,k}}{\Delta x}$$
$$-\frac{\tilde{v}^{n+1}_{i,j+1/2,k}\Delta z^{n+1}_{i,j+1/2,k}-\tilde{v}^{n+1}_{i,j-1/2,k}\Delta z^{n+1}_{i,j-1/2,k}}{\Delta y};$$
$$k = 1, 2, \ldots, N_z - 1 \tag{26}$$

In this particular case the seven diagonal system of (25) becomes homogeneous and, therefore, the unique solution of (25) becomes $q^{n+1}_{i,j,k} = 0$ identically for every i, j, k. Consequently, (21)–(23) reduce to $u^{n+1}_{i+1/2,j,k} = \tilde{u}^{n+1}_{i+1/2,j,k}$, $v^{n+1}_{i,j+1/2,k} = \tilde{v}^{n+1}_{i,j+1/2,k}$, and $w^{n+1}_{i,j,k+1/2} = \tilde{w}^{n+1}_{i,j,k+1/2}$ that is the hydrostatic solution that is obtained with the method described by Casulli and Cattani (1994).

Another important property of the present formulation arises from the fact that for $N_z = 1$ the vertical spacing Δz represents the total water depth, and the hydrodynamic pressure is identically zero. Moreover, one can easily verify that this algorithm reduces to a two-dimensional (2D) numerical method that is consistent with the 2D, vertically integrated shallow water equations and that, for $\theta = 1$, yields the method described by Casulli (1990). This property of the algorithm leads to a computer code that can be used for both 3D problems as well as 2D problems. More importantly, when the 3D model is applied to a typical coastal plain tidal embayment characterized by deep channels connected to large and flat shallow areas, a great savings in computing is achieved because the deep channels are correctly represented in three dimensions whereas the flat shallow areas are represented only in two dimensions.

The foregoing algorithm also applies to the Reynolds-averaged Navier-Stokes equations in curvilinear coordinates and with σ coordinate in the vertical (Blumberg and Mellor 1987; Mahadevan et al. 1996b).

Though a rigorous stability analysis is not yet available, for $\theta \geq 1/2$ the stability of this scheme has been observed to be independent of the celerity, bottom friction, wind stress, and vertical eddy viscosity. A mild limitation on the time step is

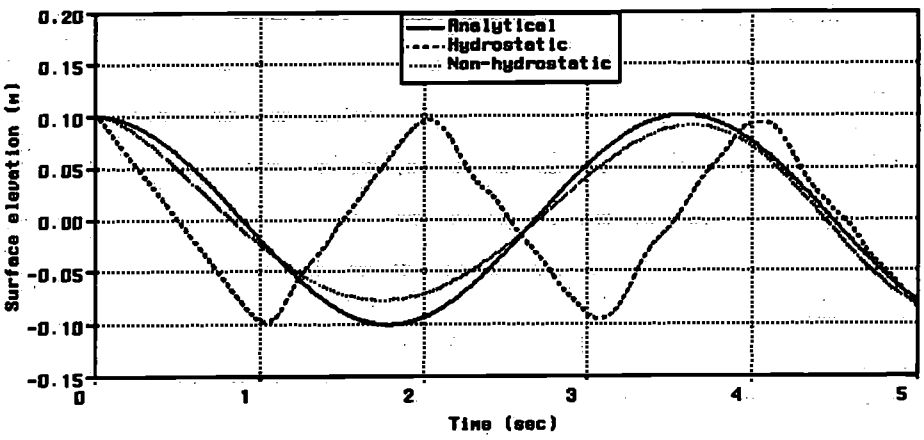

FIG. 1. Free-Surface Waves of Small Amplitude

imposed by the explicit discretization of the baroclinic pressure gradient and horizontal eddy viscosity terms.

APPLICATIONS

This section shows the importance of the nonhydrostatic pressure for various situations that are relevant for applications in civil engineering. In general, one might argue that hydrostatic models are capable of predicting the vertical structure of mainly horizontal flow. However, if the vertical component of the velocity vector is also of some importance, then hydrostatic models will not be accurate. A few examples will illustrate this point.

The first example deals with the nonbreaking waves resulting for a relatively large ratio of total depth $H = h + \eta$ to the wave length λ. In such a case the hydrostatic pressure assumption does not apply and, for sufficiently small-wave amplitude, the wave celerity c is better approximated by the following dispersion relation:

$$c = \sqrt{\frac{g\lambda}{2\pi} \tanh\left(\frac{2\pi H}{\lambda}\right)} \tag{27}$$

A square basin of length $L = 10$ m and depth $h = 10$ m is discretized with 400 square cells of equal sides $\Delta x = \Delta z_k = 0.5$ m. Starting with zero initial velocity the flow is driven by an initial free surface of constant slope $\eta = 0.02x - 0.1$. By neglecting bottom friction, horizontal, and vertical viscosity, the calculation is carried out with a small time step $\Delta t = 0.001$ s. The choice of such a small time step enables higher accuracy since, in this example, the flow is fully nonhydrostatic. The expected solution consists of a standing wave of length $\lambda = 2L$ and frequency $f = c/\lambda$, where c is given by the preceding dispersion relation. Fig. 1 shows the water surface elevation at $x = 10$ m, clearly indicating that the wave speed computed without the hydrostatic approximation is in much better agreement with the wave speed estimated analytically by the dispersion relation (27). Accordingly, the resulting flow structure is very different for the two runs [Figs. 2(a,b)].

The second example is concerned with spatial evolution of steep waves propagating over a longshore bar. To this purpose we refer to the Scheldt Flume experiment carried at Delft Hydraulics (Beji and Battijes 1994). The flume has an overall length of 30 m. The bottom profile is shown in Fig. 3. The still water level over the horizontal bottom was 0.4 m and reduced to 0.1 m over a submerged trapezoidal bar. At the end of the flume a plane beach with a 1:25 slope serves as a wave absorber. The computational domain is discretized using $\Delta x = \Delta z_k = 1$ cm. A sinusoidal wave of 1-cm amplitude and period $T = 2.02$ s is specified at the left open boundary. The time step chosen for this example is $\Delta t = 0.01$ s. The resulting water surface elevation at three stations located at 2, 13.5, and 15.7 m from the open boundary is compared against the measurements obtained by M. W. Dingemans (private communication, 1993) at Delft Hydraulics on a similar experiment in Figs. 4–6, respectively. This example illustrates the potential of the present model in dealing with complex wave problems that were, so far, only solved by means of the Boussinesq-type models (Beji and Battijes 1994). For this example the hydrostatic solution is totally different and, of course, unrealistic.

The third example is concerned with the so-called "lock-exchange" problem. A rectangular basin of length $L = 2$ m and depth $h = 0.3$ m is initially filled with two fluids with different densities $\rho_1 = 1.03$ and $\rho_2 = 1.0$, separated by a vertical dam

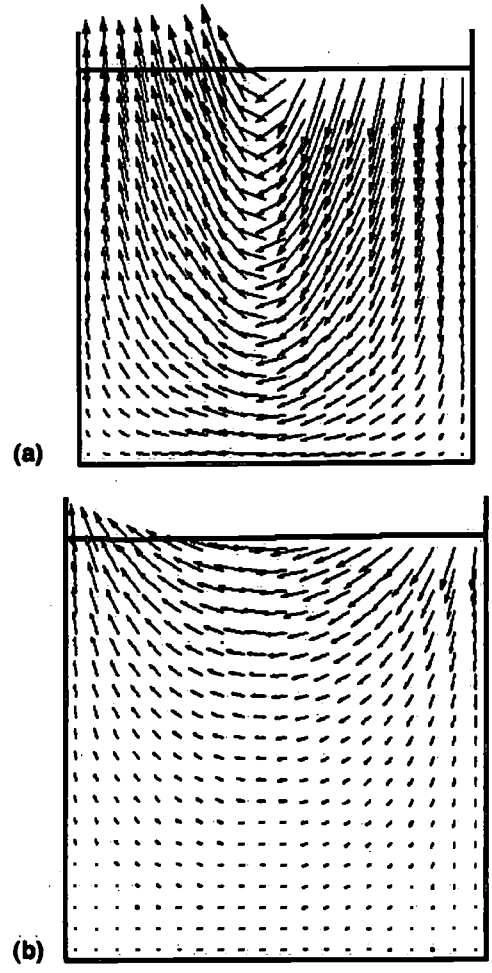

FIG. 2. Circulation in Oscillating Basin: (a) with Hydrostatic Approximation; (b) without Hydrostatic Approximation

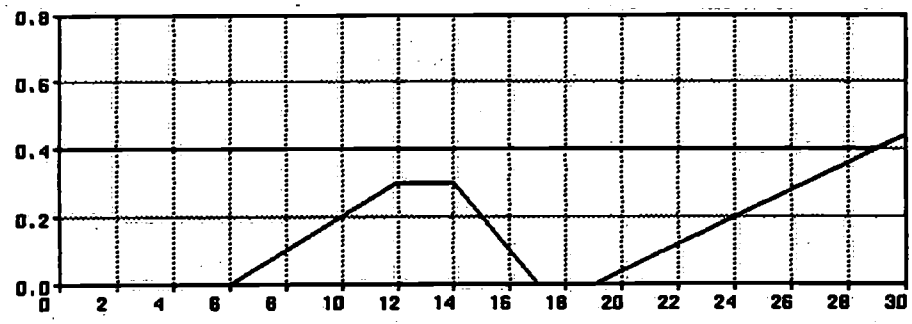

FIG. 3. Wave Flume Geometry

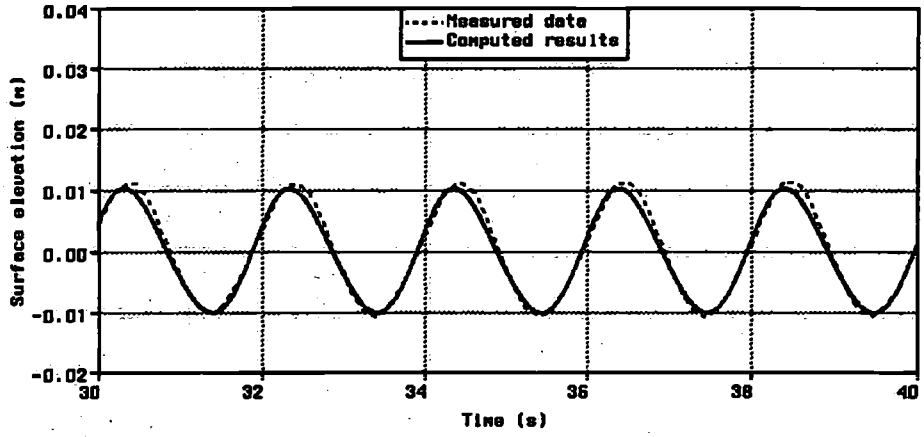

FIG. 4. Water Surface Elevation at 2 m from Open Boundary

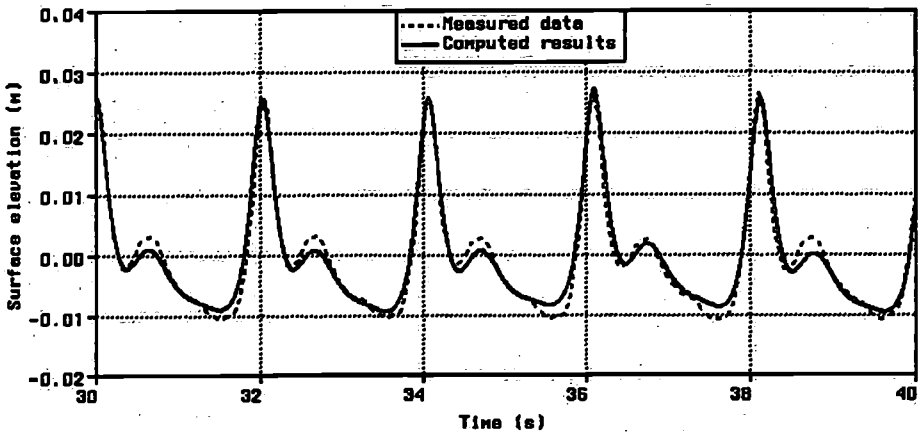

FIG. 5. Water Surface Elevation at 13.5 m from Open Boundary

located centrally in the basin. A constant eddy viscosity $\nu^h = \nu^v = 10^{-4}$ m^2/s has been used to prevent the development of interfacial instabilities. The governing equations now include an equation for the density and the baroclinic pressure terms in the momentum equations. The density equation is discretized with a semi-implicit Eulerian-Lagrangian method whereas the baroclinic terms are discretized explicitly. The bottom friction is neglected, the initial velocities are zero, and the discretization parameters are taken to be $\Delta x = \Delta z_k = 1$ cm and $\Delta t = 0.01$ s. Once the dam is removed the resulting hydrostatic solution shows the development of two discontinuities moving in opposite directions [Fig. 7(a)]. Once again, the nonhydrostatic solution obtained for this example is quite different as shown in Fig. 7(b). In the hydrostatic case the shape of the front is rectangular, whereas in the nonhydrostatic case the shape is rounded. Following Turner (1973), the latter is a more realistic shape of the interface. In Simpson (1987) several pictures of density-driven interfacial currents are given; none of them giving front shapes similar to Fig. 7(a).

The fourth example is concerned with a fully 3D problem. A square basin with sides of 100 m and depth of 10 m is filled with a fluid whose initial free surface has the shape of a Gaussian surface with the peak located at the center of the basin $\eta(x, y, 0) = e^{-0.1(x^2+y^2)}$. The bottom friction, horizontal, and vertical viscosity have been neglected. The discretization parameters are $\Delta x = \Delta y = \Delta z_k = 1$ m so that the computational domain is filled with 100,000 finite difference cells. The time step is taken to be $\Delta t = 0.1$ s. At time $t = 10$ s the original wave is reflected against the side walls and is back at the center of the basin according to the celerity that, in this case, is about 10 m/s [Fig. 8(a)]. Fig. 8(b) shows a completely different wave pattern at time $t = 10$ s obtained for the same problem without the hydrostatic approximation. Thus, the hydrostatic solution cannot be correct.

Finally, the present method has also been applied to simulate the tidal flow in the Lagoon of Venice in a situation where the hydrostatic approximation is valid. The Lagoon of Venice covers an area of about 50 km^2 and consists of several inter-

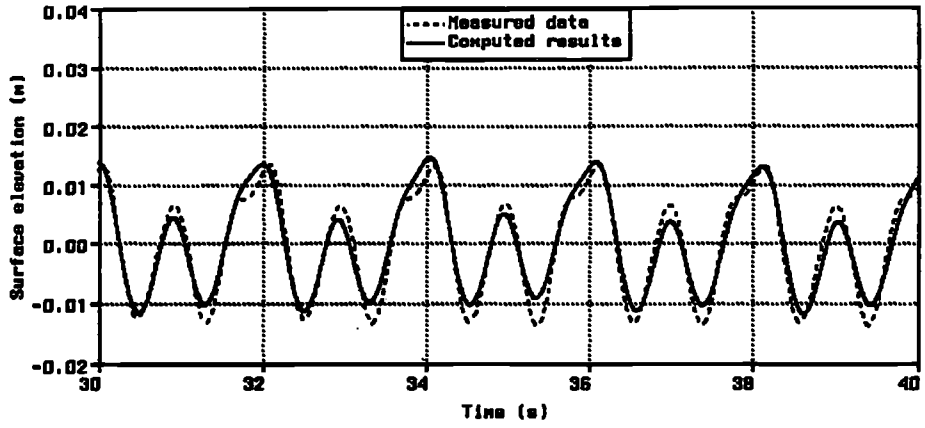

FIG. 6. Water Surface Elevation at 15.7 m from Open Boundary

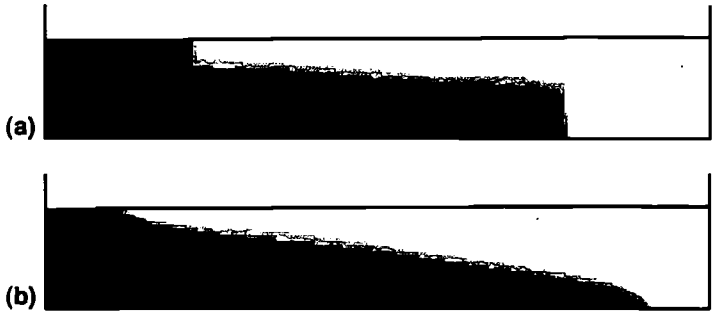

FIG. 7. Baroclinic Circulation: (a) with Hydrostatic Approximation at $t = 6$ s; (b) without Hydrostatic Approximation at $t = 6$ s

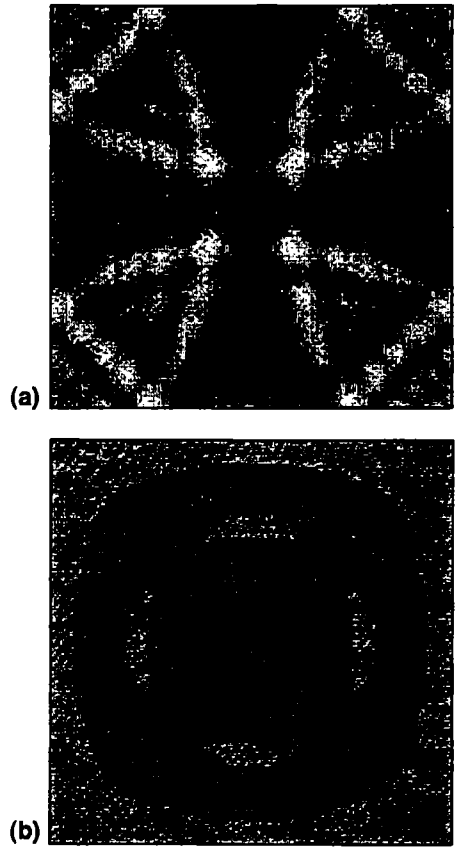

FIG. 8. Wave Pattern Generated: (a) with Hydrostatic Approximation; (b) without Hydrostatic Approximation

connected narrow channels with a maximum width of 1 km and up to 50-m deep encircling large and flat shallow areas. The lagoon is connected to the Adriatic Sea through three narrow inlets, namely Lido, Malamocco, and Chioggia. The city of Venice is located in the lagoon near the Lido inlet. A considerable portion of the Lagoon of Venice consists of tidal flats, and proper treatment of flooding and drying is essential. The tidal amplitudes in the Adriatic Sea are about 0.4 m. Tides propagate from the Adriatic Sea into the lagoon through the three inlets. The lagoon has been covered with a 672 by 846 by 200 finite difference mesh of $\Delta x = \Delta y = 50$ m and with the maximum Δz being 0.25 m. Thus, the total number of grid points is 113,702,400, but only 1,637,508 of these are active. This fine computational mesh allows for a very accurate description of the tree-like structure of the main channels as shown in Fig. 9. The fluid is assumed homogeneous (unstratified) and is driven at the three inlets where an M_2 tide of 0.4-m amplitude and 12-lunar-h period has been specified. With an integration time step $\Delta t = 15$ min the central processing unit time required to run one tidal cycle on a DEC 600 5/333 workstation is 41 min under the assumption of hydrostatic flow. Calculating the nonhydrostatic flow requires only 16 min of additional central processing unit time per tidal cycle. This is justified by the larger horizontal scale over the vertical scale of this example. Consequently, one iteration of a preconditioned conjugate gradient method is sufficient to solve the seven diagonal system [(25)] at each time step and, accordingly, the calculations with and without the hydrostatic approximation gives similar results (Fig. 10). The use of such a large time step has been made to emphasize the fact that the present model remains stable even for exceptionally large Courant numbers, but, of course, a smaller time step should be used if higher time accuracy is desired.

CONCLUSIONS

A finite difference method for solving the 3D Reynolds-averaged Navier-Stokes quations has been outlined. The implicit coupling between the momentum and the free-surface equation renders this scheme unconditionally stable with respect to the surface wave speed. For most geophysical applications, where the horizontal space steps are to be taken much larger than the vertical ones, the bottom friction and the vertical viscosity terms also have been discretized implicitly. Moreover, since the hydrodynamic pressure is much smaller than the hydrostatic pressure in geophysical flows, a further improvement in computational efficiency has been achieved by decoupling the hydrostatic from the hydrodynamic pressure. Thus the hydrostatic pressure is determined by solving a five diagonal linear system defined over the 2D x-y-domain. To determine the hydrodynamic pressure, fewer iterations on a larger seven diagonal system are sufficient.

The computational examples given in this paper show that this algorithm is suitable for accurate simulation of geophysical flows as well as practical engineering problems charac-

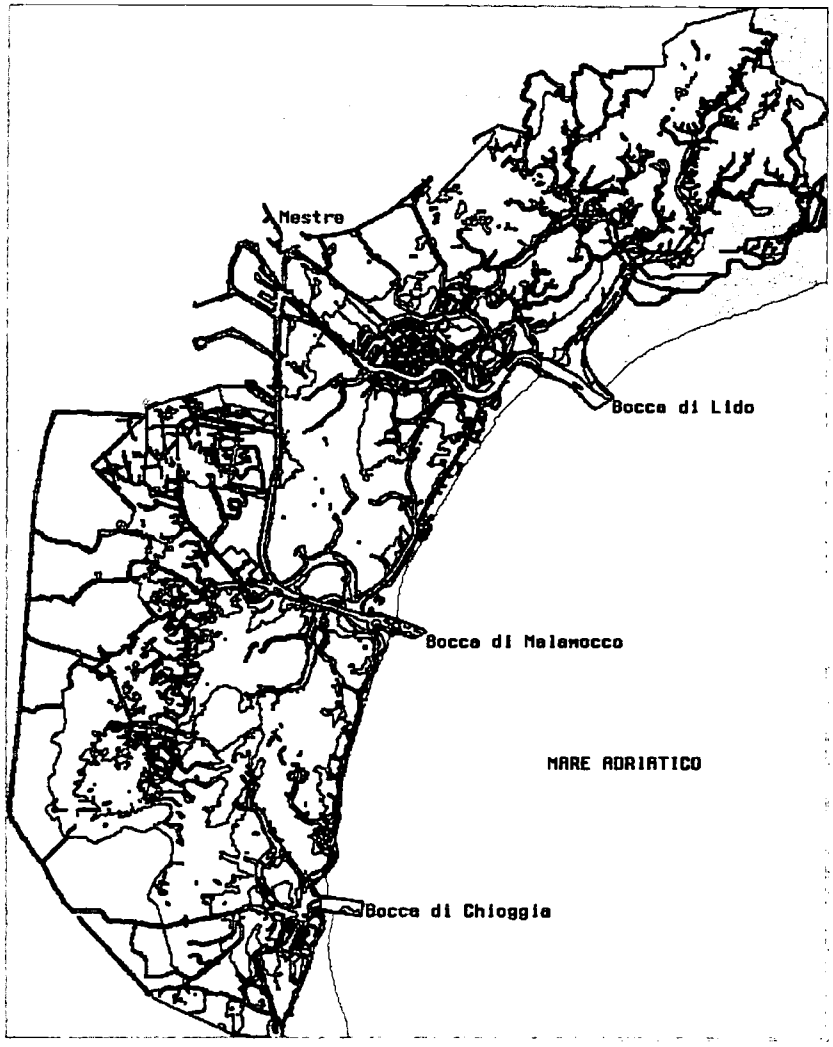

FIG. 9. High Resolution of Lagoon of Venice

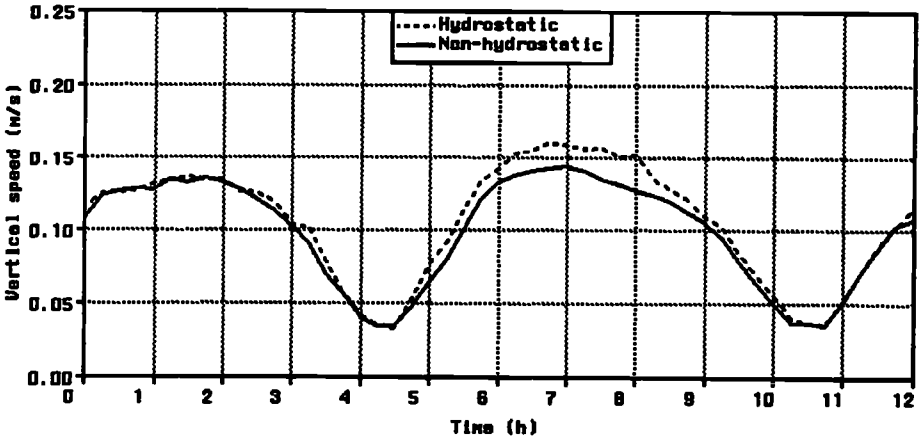

FIG. 10. Maximum Vertical Speed over Tidal Cycle

terized by waves or other phenomena for which the hydrostatic pressure alone is insufficient to obtain correct simulations. Several other examples, such as local outfalls, selective withdrawal, flow in the vicinity of structures (like weirs), medium waves in harbors, tidal flows in estuaries, all produced excellent results without extensive tuning of model parameters. It can be concluded that this method enhances the range of problems that can be solved by computational methods for free-surface flows.

APPENDIX. REFERENCES

Beji, S., and Battijes, J. A. (1994). "Numerical simulation of nonlinear waves propagation over a bar." *Coast. Engrg.*, 23(1/2), 1–16.

Benqué, J. P., Cunge, J. A., Fuillet, J., Hauguel, A., and Holly, F. M. (1982). "New method of tidal current computation." *J. Wtrwy., Port, Coast., and Oc. Div.*, ASCE, 108(3), 396–417.

Blumberg, A. F., and Mellor, G. L. (1987). "A description of a three dimensional coastal ocean circulation model." *Three dimensional coastal ocean circulation models, coastal and estuarine sciences,*

N. S. Heaps, ed., Vol. 4, Am. Geophys. Union, Washington, D.C., 1–16.
Bulgarelli, U., Casulli, V., and Greenspan, D. (1984). *Pressure methods for the numerical solution of free surface fluid flows*. Pineridge Press, Swansea, Wales, U.K.
Casulli, V. (1990). "Semi-implicit finite difference methods for the two-dimensional shallow water equations." *J. Computational Phys.*, 86(1), 56–74.
Casulli, V. (1995). "Recent developments in semi-implicit numerical methods for free surface hydrodynamics." *Advances in hydro-science and engineering*, Vol. 2, Tsinghua Univ. Press, Beijing, PRC, 2174–2181.
Casulli, V., and Cattani, E. (1994). "Stability, accuracy and efficiency of a semi-implicit method for three-dimensional shallow water flow." *Comp. and Math. with Applications*, 27(4), 99–112.
Casulli, V., and Cheng, R. T. (1992). "Semi-implicit finite difference methods for three-dimensional shallow water flow." *Int. J. for Numer. Methods in Fluids*, 15(6), 629–648.
Casulli, V., and Stelling, G. S. (1996). "Simulation of three-dimensional, non-hydrostatic free-surface flows for estuaries and coastal seas." *Proc., 4th Int. Conf. on Estuarine and Coast. Modeling*, M. L. Spaulding and R. T. Cheng, eds., ASCE, Reston, Va., 1–12.
Cox, M. D. (1984). "A primitive equation, three-dimensional model of the ocean." *GFDL Oc. Group Tech. Rep. No. 1*, Geophys. Fluid Dyn. Lab./Princeton Univ.
de Goede, E. (1991). "A time splitting method for three dimensional shallow water equations." *Int. J. Numer. Methods in Fluids*, 13(4), 519–534.
Harlow, F. H., and Welch, J. E. (1965). "Numerical calculation of time dependent viscous, incompressible flow." *Phys. of Fluids*, 8(12), 2182–2189.
Leendertse, J. J. (1967). "Aspects of a computational method for long-period water wave propagation." *Memo. RM-5294-PR*, The RAND Corp., Santa Monica, Calif.
Leendertse, J. J. (1989). "A new approach to three-dimensional free-surface flow modelling." *Memo. R-3712-NETH/RC*, The RAND Corp., Santa Monica, Calif.
Madala, R. V., and Piacsek, S. A. (1977). "A semi-implicit numerical model for baroclinic oceans." *J. Computational Phys.*, 23(2), 167–178.
Mahadevan, A., Oliger, J., and Street, R. (1996a). "A nonhydrostatic mesoscale ocean model. Part I: Well posedness and scaling." *J. Phys. Oceanography*, 26(9), 1868–1880.
Mahadevan, A., Oliger, J., and Street, R. (1996b). "A nonhydrostatic mesoscale ocean model. Part II: Numerical implementation." *J. Phys. Oceanography*, 26(9), 1881–1900.
Pedlosky, J. (1979). *Geophysical fluid dynamics*. Springer-Verlag New York, Inc., New York, N.Y.
Simpson, J. E. (1987). *Gravity currents in the environment and in the laboratory*. Ellis Horwood, Ltd., Chichester, England.
Stelling, G. S. (1983). "On the construction of computational methods for shallow water flow problems." *No. 35*, Rijkswaterstaat Communications, The Hague, The Netherlands.
Stelling, G. S., and Leendertse, J. J. (1992). "Approximation of convective processes by cyclic AOI methods." *Proc., 2nd Int. Conf. on Estuarine and Coast. Modeling*, M. L. Spaulding, K. Bedford, A. Blumberg, R. T. Cheng, and C. Swanson, eds., ASCE, Reston, Va., 771–782.
Tome, M. F., and McKee, S. (1994). "GENSMAC: A computational marker and cell method for free surface flows in general domains." *J. Computational Phys.*, 110(1), 171–186.
Turner, J. S. (1973). *Buoyancy effect in fluids*. Cambridge Univ. Press, New York, N.Y.
Wilders, P., Stelling, G. S., Stijn, van T. L., and Fokkema, G. A. (1988). "A fully implicit splitting method for accurate tidal computation." *Int. J. Numer. Methods in Engrg.*, 26(12), 2707–2721.